

## Electron emission properties of relaxation-induced traps in InAs/GaAs quantum dots and the effect of electronic band structure

J. F. Chen and J. S. Wang

Citation: [Journal of Applied Physics](#) **102**, 043705 (2007); doi: 10.1063/1.2770817

View online: <http://dx.doi.org/10.1063/1.2770817>

View Table of Contents: <http://scitation.aip.org/content/aip/journal/jap/102/4?ver=pdfcov>

Published by the [AIP Publishing](#)

---

### Articles you may be interested in

[Characterization of electron emission from relaxed InAs quantum dots capped with InGaAs](#)  
J. Appl. Phys. **98**, 013716 (2005); 10.1063/1.1957124

[Carrier distribution and relaxation-induced defects of InAs/GaAs quantum dots](#)  
Appl. Phys. Lett. **77**, 3027 (2000); 10.1063/1.1323735

[Characterization of electron trap states due to InAs quantum dots in GaAs](#)  
Appl. Phys. Lett. **76**, 2916 (2000); 10.1063/1.126516

[Observation of carrier depletion and emission effects on capacitance dispersion in relaxed In 0.2 Ga 0.8 As/GaAs quantum wells](#)  
Appl. Phys. Lett. **75**, 2461 (1999); 10.1063/1.125048

[Electrical characterization of partially relaxed In x Ga 1x As /GaAs multiple quantum well structures](#)  
Appl. Phys. Lett. **70**, 3284 (1997); 10.1063/1.118428

---



## Re-register for Table of Content Alerts

Create a profile.



Sign up today!



# Electron emission properties of relaxation-induced traps in InAs/GaAs quantum dots and the effect of electronic band structure

J. F. Chen<sup>a)</sup> and J. S. Wang

*Department of Electrophysics, National Chiao Tung University, Hsinchu, Taiwan, Republic of China*

(Received 9 May 2007; accepted 3 July 2007; published online 22 August 2007)

The electron-emission properties of relaxation-induced traps in InAs/GaAs quantum dots (QDs) are studied in detail using capacitance-voltage ( $C$ - $V$ ) profiling and bias-dependent deep-level transient spectroscopy. Strain relaxation is shown to induce a threading-dislocation-related trap in the top GaAs layer and a misfit-dislocation-related trap near the QD. The threading trap decreases its electron-emission energy from 0.63 to 0.36 eV from sample surface toward the QD, whereas the misfit trap gradually increases its electron-emission energy from 0.28 to 0.42 eV from near the QD toward the GaAs bottom layer, indicating that both traps near the QD have lower electron-emission energies. Hence, the emission-energy change is attributed to the related traps across the QD interface where a band offset exists. The  $C$ - $V$  profiling at 300 K shows extended carrier depletion near the QD. As temperature is increased, an electron-emission peak emerges at the QD followed by a prominent peak, suggesting that the trap responsible for the prominent peak lies in energy below the QD electron ground state. From a simulation, this trap is identified to be the misfit trap located at the QD and at the observed emission energy below the GaAs conduction band. Based on the energy location of this trap, we deduce a possible mode of strain relaxation. © 2007 American Institute of Physics. [DOI: 10.1063/1.2770817]

## I. INTRODUCTION

InAs/GaAs self-assembled quantum dots<sup>1-9</sup> (QDs) have recently attracted considerable attention for both theoretical and experimental studies due to promising technological applications.<sup>10-14</sup> Many works have focused on experimentally determining the electronic band structure of the QD (Refs. 15-20) by analyzing electron emission from the QD. However, this emission time is very short and difficult to resolve probably due to the presence of significant tunneling.<sup>15,19,20</sup> On the other hand, deep traps with their strongly localized wave functions have been proposed as local probes for characterizing electronic band structure.<sup>22-24</sup> When InAs thickness is increased beyond the critical thickness ( $\sim 3$  ML),<sup>21</sup> strain is relaxed by the formation of misfit dislocations confined near relaxation interface. This trap was previously shown to be point-defect-like<sup>25</sup> because its capacitance-time transience exhibits an exponential function. Hence, it would be worthwhile to explore the possibility of using this trap as a probe. Furthermore, understanding the electron-emission properties of this trap may also provide valuable information on strain relaxation. Therefore, in this work, the electron-emission properties of relaxation-induced traps in InAs QDs are investigated in detail by using capacitance-voltage ( $C$ - $V$ ) profiling and deep-level transient spectroscopy (DLTS) with small step voltages.

Among many electrical characterizations, DLTS is very convenient for evaluating the carrier-emission properties of defect traps. However, when the probed sample is not of a simple bulk structure, analyzing DLTS spectra is difficult because the emission parameters are affected by band struc-

ture, and thus bias dependent. This task is even more difficult when multiple traps are present. This work has demonstrated an important effect of electronic band structure. Selecting a small step voltage was necessary to resolve the DLTS spectra of relaxation-induced traps. Aided by  $C$ - $V$  profiling at elevated temperatures and a band structure simulation, we were able to obtain important information on the electron-emission parameters of two traps related to threading and misfit dislocations, respectively.

## II. EXPERIMENTS

The InAs/GaAs QD samples studied here were grown on  $n^+$ -GaAs (100) substrates by solid source molecular beam epitaxy in a Riber Epineat machine. The QDs were formed in Stranski-Krastanow growth mode by depositing the InAs layer at 490 °C. The QDs structure is sandwiched between two 0.3  $\mu\text{m}$ -thick Si-doped GaAs ( $\sim 6 \times 10^{16} \text{ cm}^{-3}$ ) layers for electrical characterizations. Detailed growth of the QD samples can be found elsewhere.<sup>26</sup> A typical QD sheet density about  $3 \times 10^{10} \text{ cm}^{-2}$  was observed by atomic force microscopy images. Schottky diodes were realized by evaporating Al on sample surface with a dot diameter of 1500  $\mu\text{m}$ . Photoluminescence (PL) measurements were carried out using a double frequency yttrium-aluminum-garnet:Nd laser at 532 nm. A HP 4194A gain phase analyzer was used for  $C$ - $V$  profiling.

## III. MEASUREMENT AND RESULTS

### A. DLTS spectra of relaxed QDs

In the previous transmission electron microscopy studies,<sup>21</sup> strain in InAs QDs was shown to relax by the induction of threading dislocations in the top GaAs layer and

<sup>a)</sup>Electronic mail: jfchen@cc.nctu.edu.tw

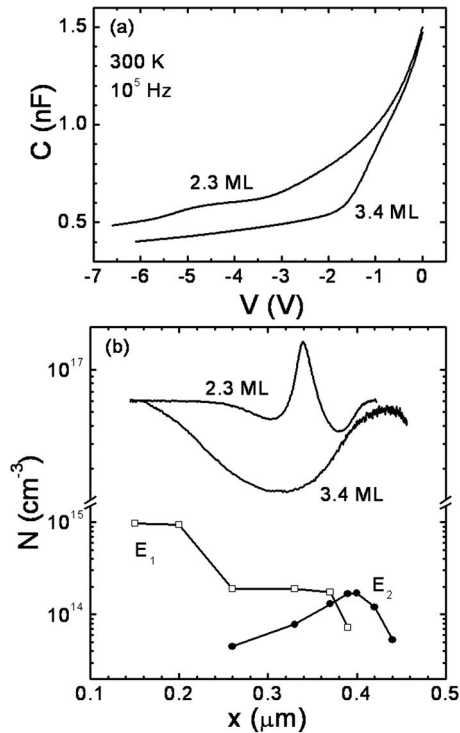


FIG. 1. (a) 300-K  $C$ - $V$  and (b) concentration profiles measured at  $10^5$  Hz for the nonrelaxed 2.3 ML and relaxed 3.4 ML samples. Strain relaxation causes carrier depletion near the dot ( $0.3 \mu\text{m}$ ) and neighboring GaAs layers by the generation of two traps, E1 and E2, related to the threading and misfit dislocations, respectively. Their concentrations, determined from the DLTS spectra in Fig. 3, show that the E1 trap is located in the top GaAs layer and the E2 trap is located near the QD.

misfit dislocations near the QDs. The threading dislocations which propagate from the QDs to the sample surface are likely generated by the gliding process of interfacial dislocations due to elastic strain acting as a shear stress.<sup>27,28</sup> In contrast, the misfit dislocations do not propagate into the GaAs layers but are confined near the QD, suggesting a bending of the misfit dislocations toward the QD interface by strain. Similar confinement of misfit dislocations has been observed in relaxed InGaAs/GaAs heterostructures.<sup>28</sup>

Figures 1(a) and 1(b) show the 300-K  $C$ - $V$  and the converted concentration profiles of InAs QD samples with InAs thicknesses of 2.3 and 3.4 ML, respectively, measured at  $10^5$  Hz. The latter sample is relaxed because the InAs thickness exceeds the critical thickness of  $\sim 3$  ML.<sup>21</sup> While the 2.3 ML sample shows strong electron accumulation, the relaxed sample exhibits carrier depletion at the dots ( $0.3 \mu\text{m}$ ) and neighboring GaAs layers. Hence, strain relaxation must induce electron traps to deplete the QDs. DLTS measurements were used to reveal the traps. Figure 2 shows the obtained spectra of the 2.3 and 3.4 ML samples, along with a 1.1 ML InAs sample which is of a quantum-well structure because QD has not formed. The sweeping voltages are as indicated. While the 1.1 and 2.3 ML samples display no traps, the 3.4 ML sample exhibits a broad signal at low temperature superimposed upon a background signal, suggesting the presence of significant relaxation-induced traps. Figure 3 shows that when step voltage is reduced to  $-0.5$  V (superimposed upon a quiescent bias from 0 to  $-4$  V), the spec-

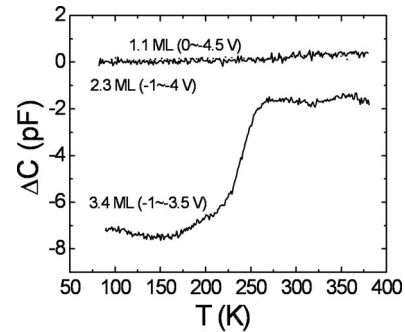


FIG. 2. DLTS spectra of the 1.1 ML InAs quantum-well sample, nonrelaxed 2.3 ML, and relaxed 3.4 ML InAs QDs samples under various sweeping voltages as indicated. Strain relaxation causes a broad signal at low temperatures superimposed on a high-temperature background signal, which can be resolved into two major traps in Fig. 3 when a small step voltage is selected.

trum can be well resolved into two prominent traps, E1 from  $0/-0.5$  to  $-3.5/-4$  V and E2 from  $-1/-1.5$  to  $-4/-4.5$  V. The rate window is 8.6 ms and filling pulse time is set at 30 ms to ensure the peak-height saturation of the E2 trap. As guided by the dash lines, the peak temperature of E1 (E2) shifts toward a lower (higher) temperature as reverse bias is increased. This strong bias dependence can explain the broad spectrum in Fig. 2. As shown in Fig. 3, the E2 traps for  $-1/-1.5$  and  $-1.5/-2$  V are rather asymmetric with a broad low-temperature tail, and thus their emission energies cannot be determined accurately. Figure 4 shows the corresponding Arrhenius plots of the traps, from which the activation energies and capture cross sections are obtained.

Given the DLTS spectra in Fig. 3 and the  $C$ - $V$  curve in Fig. 1(a), the concentrations and spatial locations of the traps

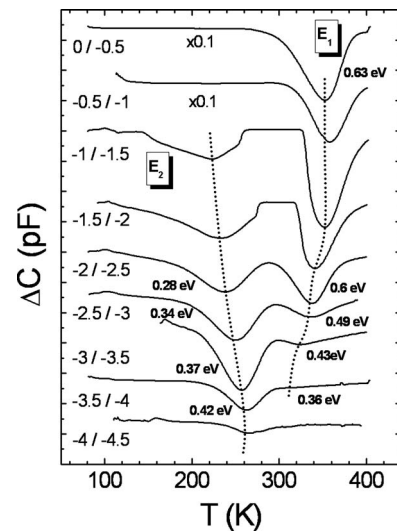


FIG. 3. DLTS spectra of the relaxed 3.4 ML sample, showing two traps: the E1 trap is associated with the threading dislocations in the top GaAs layer and the E2 trap is associated with the misfit dislocations near the QD. With increasing reverse quiescent bias, the peak temperature of the E1 (E2) trap shifts toward a lower (higher) temperature, reflecting smaller electron-emission energies for both the traps near the QD. This effect is attributed to the related traps across the QD interface where a band offset locates. The E2 spectra from  $-1/-1.5$  to  $-2.5/-3$  V is asymmetric with a very broad low-temperature tail, suggesting the presence of continuous energy states below the GaAs CB edge, to which electrons are emitted from the E2 trap. The continuous states are attributed to the QD electron states.

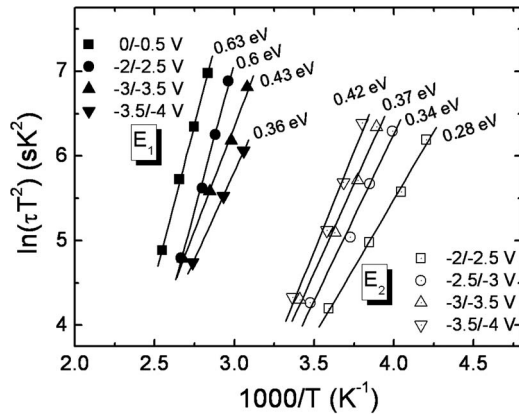


FIG. 4. Arrhenius plots of the E1 and E2 traps at different sweeping voltages. The electron-emission energies are also indicated in the DLTS spectra in Fig. 3.

are evaluated, as shown in Fig. 1(b). The concentration is determined from the expression  $(2\Delta C/C)N$ , where  $\Delta C$  is the peak intensity of the related trap and  $N$  is the background concentration  $6 \times 10^{16} \text{ cm}^{-3}$ . The spatial location is simply obtained from the edge of depletion region (EOD) from the  $C$ - $V$  curve. For example, for the E1 trap observed in 0/-0.5 V, a middle bias -0.25 V is used to find the EOD. A trap will donate carriers only when Fermi level crosses it. However, at this point, due to the energetic depth of the trap, the EOD is deeper than the crossing point, and thus the obtained location is deeper than the actual location of the trap. From a simple simulation (to be shown), a trap that is located at the QDs ( $0.3 \mu\text{m}$ ) and at  $0.35 \text{ eV}$  below the GaAs conduction-band (CB) edge will show its emission signal at  $0.39 \mu\text{m}$ . Thus, the depth  $0.39 \mu\text{m}$  in Fig. 1(b) can be roughly treated as the location of the QDs. Hence, the E1 trap is located from the sample surface to a depth near the QDs. Its concentration gradually decreases from the surface toward the QD. This spatial distribution correlates with that of the threading dislocations, and thus the E1 trap is attributed to the threading dislocations. The E2 trap is located in the vicinity of the QDs; its concentration gradually increases from the top GaAs layer near the QDs, reaches a maximum at the QD, and then rapidly decreases toward the lower GaAs layer. This spatial distribution leads us to attribute the E2 trap to the misfit dislocations.

## B. Properties of the threading trap

As shown in Figs. 3 and 4, the electron-emission energy of the E1 trap decreases from  $0.63 \text{ eV}$  ( $\alpha=3.9 \times 10^{-15} \text{ cm}^{-2}$ ) for 0/-0.5 V to  $0.36 \text{ eV}$  ( $\sigma=1.9 \times 10^{-16} \text{ cm}^{-2}$ ) for -3.5/-4 V, suggesting a smaller electron-emission energy near the QDs. The DLTS peak height of this trap shows no saturation even when filling pulse duration time is increased to 100 ms. This feature is consistent with the capacitance-time transience of the traps associated with threading dislocations, which exhibits a logarithmic function,<sup>27,28</sup> characteristic of Coulombic repulsion of the carriers captured at the traps along with the linearly arrayed dislocation lines.<sup>27</sup> This trap is believed to be the ED1 ( $0.68 \text{ eV}$ ), reported by Wosinski<sup>27</sup> from studying plas-

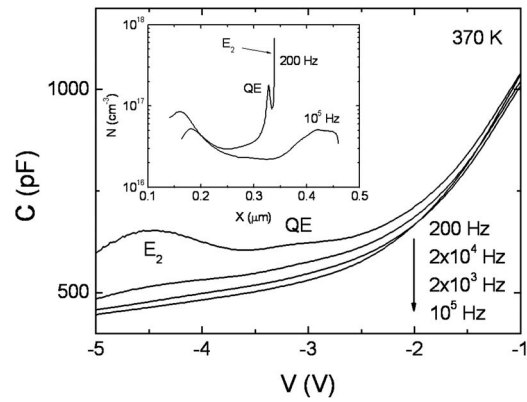


FIG. 5.  $C$ - $V$  spectra and the corresponding concentration profiles (in the inset) of the relaxed 3.4 ML sample, measured at 370 K. When frequency is reduced to 200 Hz, the  $C$ - $V$  spectra show a  $C$  plateau, corresponding to an electron-emission peak at the QD, and a  $C$  protrusion, corresponding to electron emission from the E2 trap.

tically deformed GaAs, and the trap at  $0.58 \text{ eV}$  observed in InGaAs/GaAs by Watson *et al.*<sup>29</sup> who assigned it to the cores of  $\alpha$ -type dislocations. The electron-emission energy obtained by Watson *et al.*<sup>29</sup> is smaller than that by the Wosinski.<sup>27</sup> Watson *et al.*<sup>29</sup> explained this by the threading dislocations in the InGaAs side which has a smaller band gap, as relative to GaAs. He suggested that the trap was probably tied to the valence-band edge and thus the emission-energy difference might be the band gap difference between GaAs and InGaAs. This band structure effect can explain the decrease of the electron-emission energy of the E1 trap. A trap generally decreases its emission energy as the band gap of the host material is reduced. For example, Irvine and Palmer<sup>30</sup> have shown an electron-emission-energy decrease in EL2 from  $0.84$  to  $0.62$  as  $x$  increases from 0 to 0.18 for an  $\text{In}_x\text{Ga}_{1-x}\text{As}$  layer grown on GaAs. Hence, the electron-emission-energy change may reflect the energy band structure of the host material. Further investigation is needed to make a quantitative argument.

## C. $C$ - $V$ profiling at elevated temperatures

As Fig. 1(b) is shown, the QD in the relaxed 3.4 ML sample is depleted of electrons. This depletion is presumably caused by the E2 trap which must lie in energy below the QD electron ground state. Due to the long emission time, electrons trapped on the E2 trap cannot follow the alternating current (ac) signal to be modulated. This depletion remains as frequency is lowered to 200 Hz. However, one may directly activate the electron emission from the trap by increasing temperature to reduce the emission time. Figure 5 shows the  $C$ - $V$  and the corresponding depth profiles (in the inset) at 370 K. The profile shows similar carrier depletion at  $10^5 \text{ Hz}$ ; however, at 200 Hz, a  $C$  plateau at around -3 V and a  $C$  protrusion at around -4.5 V emerge. The  $C$  plateau is converted to a carrier-accumulation peak centered at  $0.33 \mu\text{m}$ . This depth is close to the location ( $0.34 \mu\text{m}$ ) of the carrier-accumulation peak in the nonrelaxed 2.3 ML sample [in Fig. 1(b)], and thus the peak is considered as electron emission from the QD electron states and is designated as quantum emission (QE). The presence of the QD electron states can



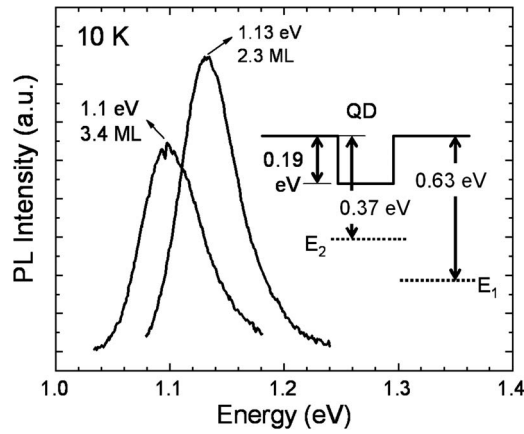


FIG. 6. 10-K PL spectra of the nonrelaxed 2.3 and relaxed 3.4 ML QD samples, showing a redshift of the QD ground emission. Strain relaxation does not severely degrade the QD quality. Also included is a schematic CB diagram showing the QD electron ground state (at 0.19 eV below the GaAs CB edge) and energetic and spatial locations of the threading trap E1 and misfit trap E2. For simplicity, the effect of electronic band structure on the electron-emission energies of both traps is not shown.

be justified from the 10-K PL spectra in Fig. 6 of the nonrelaxed 2.3 ML and the relaxed 3.4 ML samples. The 2.3 ML sample shows a QD ground emission at 1.13 eV which is redshifted to 1.1 eV in the 3.4 ML sample presumably due to an increase in dot size. The peak of the 3.4 ML sample is only slightly broader than that of the 2.3 ML sample, suggesting that strain relaxation does not destroy the QD electron ground state. Kapteyn *et al.*<sup>15</sup> reported a value of 0.19 eV for the confinement energy of InAs QD electron ground state for an QD ground emission at 1.12 eV, a value close to the emission energy of the 3.4 ML sample. Thus, the QD electron ground state is placed at 0.19 eV below the GaAs CB edge, as shown in the simplified schematic CB diagram in Fig. 6. Neglecting the effect of band structure, the energetic locations of the E1 and E2 traps are also illustrated.

#### D. Depth-profile simulation of the misfit trap

As to the  $C$  protrusion at  $-4.5$  V (in Fig. 5), it may be due to the electron emission from the E2 trap. From the DLTS data, the emission rate of the E2 trap (at 0.37 eV for  $-3/-3.5$  V) can be extrapolated to  $1.7 \times 10^3$  Hz at 370 K which is larger than the ac modulating frequency of 200 Hz, allowing for the E2 trap to be modulated. This  $C$  protrusion is seen after the QE peak, suggesting that the E2 trap lies below the QD electron ground state, consistent with the carrier-depletion effect. To see what energy level the electron-emission energy is relative to, we simulate  $C$ - $V$  profile by solving the Poisson equation for a  $n$ -type GaAs Schottky diode (a barrier height of 0.84 eV) with a background doping of  $6 \times 10^{16}$   $\text{cm}^{-3}$  and an acceptor trap of  $3 \times 10^{17}$   $\text{cm}^{-3}$  at the QD (0.3  $\mu\text{m}$ ) with a thickness of 10 nm (equivalent to a sheet concentration of  $3 \times 10^{11}$   $\text{cm}^{-2}$ ) and at 0.35 eV below the GaAs CB edge, as shown in Fig. 7(a). Figure 7(b) shows the simulated  $C$ - $V$  profiles under three conditions: the  $L$  curve represents a low ac frequency so that the trapped electron can be modulated, the  $M$  curve represents a medium frequency so that the trapped electron cannot

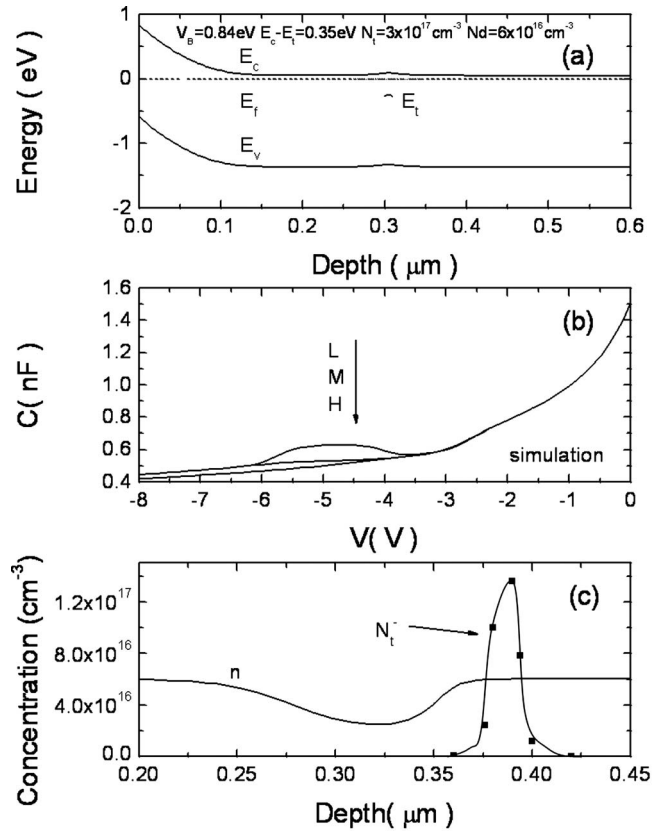


FIG. 7. (a) Energy band diagram used for simulation, assuming the presence of a trap with a concentration of  $3 \times 10^{17}$   $\text{cm}^{-3}$ , located near the QD with a thickness of 10 nm and at 0.35 eV below the GaAs CB edge. (b) Simulated  $C$ - $V$  spectra under three conditions depending upon ac frequency and dc sweeping rate: the  $L$  curve represents that the trapped electron can follow ac signal, the  $M$  curve represents that the trapped electron cannot follow ac signal but can follow dc sweeping rate, and the  $H$  curve represents that the trapped electron cannot even follow dc sweeping rate. (c) Simulated concentration profile without any trap emission (in the  $M$  condition) and concentration profile of electron emission from the E2 trap.

follow the ac signal but can follow the direct current (dc) sweeping rate, and the  $H$  curve represents that the trapped electron cannot even follow the dc sweeping rate (this condition is not satisfied during the experiment). As shown, the  $L$  and  $M$  curves are in general agreement with the experimental curves in Fig. 5 under 200 (neglecting QE plateau) and  $10^5$  Hz, respectively. Figure 7(c) shows the simulated depth profile in the  $M$  condition, illustrating carrier depletion at around 0.3  $\mu\text{m}$  which is in fair agreement with the experimental carrier depletion in Fig. 1(b). Figure 7(c) also shows the simulated concentration profile of the E2 trap using the same equation,  $(2\Delta C/C)N$  as used in Fig. 1(b), except  $\Delta C$  is taken from the difference between the  $L$  and  $M$  curves. The spatial location of the E2 trap is obtained from the  $M$  curve, which shows a nearly constant  $C$  (0.55 nF) for the observation of the  $C$  protrusion in the  $L$  curve. This constant  $C$  yields an EOD depth of 0.38  $\mu\text{m}$  which is in fair agreement with the maximum concentration (0.39  $\mu\text{m}$ ) of the E2 trap in Fig. 1(b). Therefore, the carrier depletion is mainly due to the E2 trap that is located at the QDs and at 0.37 eV below the GaAs CB edge. Note that the simulated  $C$  protrusion starts at  $-3$  V; however, the DLTS spectra show the E2 trap starting from  $-1/-1.5$  V. Thus, E2 trap probably spread into the top GaAs layer near the QDs.

### E. Mode of strain relaxation

The DLTS peak height of the E2 trap (at 0.37 eV) is found to increase and finally saturate with increasing filling pulse time. This is consistent with its capacitance-time transience which displays an exponential function,<sup>25</sup> suggesting an isolated point defect. In terms of its activation energy, it is believed the one at 0.395 eV ( $\sigma=1 \times 10^{-16} \text{ cm}^{-2}$ ) observed by Uchida *et al.*<sup>27</sup> who related it to the misfit dislocations near the relaxed InGaAs/GaAs heterojunction. Uchida *et al.*<sup>27</sup> claimed that this trap was a monolevel trap because its capture cross section was temperature independent. Recently, Yastrubchak *et al.*<sup>31</sup> reported an exponential function for a misfit-related hole trap in InGaAs/GaAs heterostructures. This trap was claimed to have a higher regularity as compared with threading dislocations. Since the E2 trap is likely a point defect and is at 0.37 eV below the GaAs CB edge, we compare it with point defects in GaAs. In terms of its energy location, it is likely EL6 ( $E_c-0.35 \text{ eV}$ ) (Ref. 32) observed in low-temperature grown GaAs, commonly considered as  $V_{\text{Ga}}\text{-As}_i$  complex. If it is indeed  $V_{\text{Ga}}\text{-As}_i$ , we can deduce a likely mode of strain relaxation. Due to underlying GaAs layer, the deposited InAs QDs are compressed laterally. At the onset of relaxation, the compressive stress in the QDs is relieved probably by the displacement of As atoms from their lattice sites, leading to excess As in the form of  $\text{As}_i$  near the QD. These  $\text{As}_i$  may react with the misfit dislocations to produce Ga vacancies ( $V_{\text{Ga}}$ ) by the interaction<sup>30</sup>:  $\text{As}_i + \text{dislocation} \rightarrow \text{dislocation climb} + V_{\text{Ga}}$ . After that, the induced  $V_{\text{Ga}}$  may interact with residual  $\text{As}_i$  and form  $\text{As}_i\text{-}V_{\text{Ga}}$  complex, leading to the spatial correlation between the E2 trap and misfits.

As Fig. 3 shown, the electron-emission energy of the E2 trap increases from 0.28 to 0.42 eV as sweeping voltage increases from  $-2/-2.5$  to  $-3.5/-4 \text{ V}$ . Additionally, the E2 spectra from  $-1/-1.5$  to  $-2.5/-3 \text{ V}$  (corresponding to a region near the QDs) contain a very broad low-temperature tail. The bias dependence of the electron-emission energy cannot be explained by a field-enhanced tunneling, since increasing the amplitude of bias would enhance emission rate and reduce electron-emission energy. This bias dependence seems to suggest a rather broad energy spectrum of the E2 trap. However, the E2 trap at 0.37 eV for  $-3/-3.5 \text{ V}$ , as well as for  $-3.5/-4 \text{ V}$ , is quite symmetric and narrow in linewidth. Also, from the simulation, electrons are emitted to the GaAs CB for these sweeping voltages. Thus, we explained the lower electron-emission energy and the low-temperature tail (from  $-1/-1.5$  to  $-2.5/-3 \text{ V}$ ) as an effect of band structure. Continuous energy states may exist below the GaAs CB edge to which electrons trapped on the E2 traps are emitted. Since they are observed in a region near the QD, the continuous states are considered as the QD electron states. Note that this trend is similar as the E1 trap; both traps show smaller electron-emission energies for a region near the QDs. Strain relaxation is expected to enhance fluctuation of the QD states, leading to a smearing of emission energies and formation of tails. The results of the present studies illustrate a significant effect of electronic band structure on the

electron-emission properties of the traps. Hence, it is possible that they can be used as probes for energy band structure of the host material.

### IV. CONCLUSIONS

We show that strain relaxation in InAs QDs can produce two electron traps: one is associated with threading dislocations in the top GaAs layer and the other is associated with misfit dislocations near the QD. The threading trap decreases its electron-emission energy from 0.63 to 0.36 eV from the sample surface toward the QD. This is explained by the trap across the QD interface where a band offset exists. By performing  $C$ - $V$  profiling at elevated temperatures, we observe a  $C$  plateau followed by a  $C$  protrusion; the plateau is identified as the electron emission from the QD and the protrusion as the electron emission from a defect trap. A simple simulation establishes that the defect trap is the misfit trap located at 0.37 eV below the GaAs conduction-band edge. In terms of its emission energy, this misfit trap is ascribed to EL6, commonly considered as  $V_{\text{Ga}}\text{-As}_i$  complex. As the E1 trap, the emission energy of the E2 trap shows a smaller electron-emission energy and a broad low-temperature tail for a region near the QD.

### ACKNOWLEDGMENTS

The authors gratefully acknowledge the National Science Council of Taiwan for financially supporting this research under Contract No. NSC-95-2112-M-009-010 and MOE, ATU program.

<sup>1</sup>F. Heinrichsdorff, M.-H. Mao, N. Kirstaedter, A. Krost, and D. Bimberg, Appl. Phys. Lett. **71**, 22 (1997).

<sup>2</sup>T. E. Nee, N. T. Yeh, P. W. Shiao, J. I. Chyi, and C. T. Lee, Jpn. J. Appl. Phys., Part 1 **38**, 605 (1999).

<sup>3</sup>D. J. Eaglesham and M. Cerullo, Phys. Rev. Lett. **64**, 1943 (1990).

<sup>4</sup>D. Leonard, K. Pond, and P. M. Petroff, Phys. Rev. B **50**, 11687 (1994).

<sup>5</sup>S. Guha, A. Madhukar, and K. C. Rajkumar, Appl. Phys. Lett. **57**, 2110 (1990).

<sup>6</sup>J. M. Moison, F. Houzay, F. Barthe, and L. Leprince, Appl. Phys. Lett. **64**, 196 (1994).

<sup>7</sup>D. J. Bottomley, Appl. Phys. Lett. **72**, 783 (1998).

<sup>8</sup>C. W. Snyder, J. F. Mansfield, and B. G. Orr, Phys. Rev. B **46**, 9551 (1992).

<sup>9</sup>D. Leonard, M. Krishnamurthy, C. M. Reaves, S. P. Denbaars, and P. M. Petroff, Appl. Phys. Lett. **63**, 3203 (1993).

<sup>10</sup>H. Shoji, K. Mukai, N. Ohtsuka, M. Sugawara, T. Uchida, and H. Ishikawa, IEEE Photonics Technol. Lett. **7**, 1385 (1995).

<sup>11</sup>G. Yusa and H. Sakaki, Electron. Lett. **32**, 491 (1996).

<sup>12</sup>N. Yokoyama, S. Muto, K. Imamura, M. Takatsu, T. Mori, Y. Sugiyama, Y. Sakuma, H. Nakao, and T. Adachi, Solid-State Electron. **40**, 505 (1996).

<sup>13</sup>Y. Arakawa and H. Sakaki, Appl. Phys. Lett. **40**, 939 (1982).

<sup>14</sup>J. C. Campbell, D. L. Huffaker, H. Deng, and D. G. Deppe, Electron. Lett. **33**, 1337 (1997).

<sup>15</sup>C. M. A. Kapteyn, F. Heinrichsdorff, O. Stier, R. Heitz, M. Grundmann, and P. Werner, Phys. Rev. B **60**, 14265 (1999).

<sup>16</sup>R. J. Luyken, A. Lorke, A. O. Govorov, J. P. Kotthaus, G. Medeiros-Riberro, and P. M. Petroff, J. Appl. Phys. **74**, 2486 (1999).

<sup>17</sup>X. Letartre, D. Stievenard, and M. Lanoo, J. Appl. Phys. **69**, 7336 (1991).

<sup>18</sup>H. L. Wang, F. H. Yang, S. L. Feng, H. J. Zhu, D. Ning, H. Wang, and X. D. Wang, Phys. Rev. B **61**, 5530 (2000).

<sup>19</sup>J. F. Chen, R. S. Hsiao, C. K. Wang, J. S. Wang, and J. Y. Chi, J. Appl. Phys. **98**, 013716 (2005).

<sup>20</sup>W. H. Chang, W. Y. Chen, M. C. Cheng, C. Y. Lai, T. M. Hsu, N. T. Yeh,

- and J. I. Chyi, Phys. Rev. B **64**, 125315 (2001).
- <sup>21</sup>J. S. Wang, J. F. Chen, J. L. Huang, P. Y. Wang, and X. J. Guo, Appl. Phys. Lett. **77**, 3027 (2000).
- <sup>22</sup>J. M. Langer and H. Heinrich, Phys. Rev. Lett. **55**, 1414 (1985).
- <sup>23</sup>D. Stievenard and S. L. Feng, Mater. Sci. Forum **38–41**, 679 (1989).
- <sup>24</sup>P. Krispin, J.-L. Lazzari, and H. Kostial, J. Appl. Phys. **84**, 6135 (1998).
- <sup>25</sup>J. F. Chen, R. S. Hsiao, W. D. Huang, Y. H. Wu, L. Chang, J. S. Wang, and J. Y. Chi, Appl. Phys. Lett. **88**, 233113 (2006).
- <sup>26</sup>J. F. Chen, R. S. Hsiao, S. H. Shih, P. Y. Wang, J. S. Wang, and J. Y. Chi, Jpn. J. Appl. Phys., Part 1 **43**, L1150 (2004).
- <sup>27</sup>T. Wosinski, J. Appl. Phys. **65**, 1566 (1989).
- <sup>28</sup>Y. Uchida, H. Kakibayashi, and S. Goto, J. Appl. Phys. **74**, 6720 (1993).
- <sup>29</sup>G. P. Watson and D. G. Ast, J. Appl. Phys. **71**, 3399 (1992).
- <sup>30</sup>A. C. Irvine and D. W. Palmer, Phys. Rev. Lett. **68**, 2168 (1992).
- <sup>31</sup>O. Yastrubchak, T. Wosinski, A. Makosa, T. Figielski, and A. L. Toth, Physica B (Amsterdam) **308–310**, 757 (2001).
- <sup>32</sup>P. W. Yu, G. D. Robinson, J. R. Sizerlove, and C. E. Stutz, Phys. Rev. B **49**, 4689 (1994).